Published in final edited form as:

J Immunol. 2022 August 01; 209(3): 435–445. doi:10.4049/jimmunol.2200030.

TOLLIP optimizes dendritic cell maturation to LPS and *Mycobacterium tuberculosis*

Sambasivan Venkatasubramanian[1], **Robyn Pryor**[1], **Courtney Plumlee**[2], **Sarah B. Cohen**[2], **Jason D. Simmons**[1], **Alexander J. Warr**[1,3], **Andrew D. Graustein**[1,4], **Aparajita Saha**[1], **Thomas R. Hawn**[1], **Kevin B. Urdahl**[2], **Javeed A. Shah**[1,4,#]

[1]University of Washington, Seattle, WA.

[2]Seattle Children's Research Institute, Seattle, WA.

[3]Baylor School of Medicine, Houston, TX.

[4]VA Puget Sound Healthcare System.

Abstract

TOLLIP is a central regulator of multiple innate immune signaling pathways, including TLR2, TLR4, IL-1R, and STING. Human TOLLIP deficiency, regulated by SNP rs5743854, is associated with increased tuberculosis (TB) risk and diminished frequency of BCG vaccine-specific CD4+ T cells in infants. How TOLLIP influences adaptive immune responses remains poorly understood. To understand the mechanistic relationship between TOLLIP and adaptive immune responses, we used human genetic and murine models to evaluate the role of TOLLIP in dendritic cell (DC) function. In healthy volunteers, TOLLIP SNP rs5743854 G allele was associated with decreased *TOLLIP* mRNA and protein expression in DCs, along with LPS-induced IL-12 secretion in peripheral blood DC. As in human cells, LPS-stimulated, *Tollip*$^{-/-}$ bone marrow-derived murine DCs secreted less IL-12 and expressed less CD40. *Tollip* was required in lung and lymph node-resident DCs for optimal induction of MHC Class II and CD40 expression during the first 28 days of Mtb infection in mixed bone marrow chimeric mice. *Tollip*$^{-/-}$ mice developed fewer Mtb-specific CD4+ T cells 28 days after infection, nor after BCG vaccination. Furthermore, *Tollip*$^{-/-}$ DC were unable to optimally induce T cell proliferation. Together, these data support a model where TOLLIP-deficient DCs undergo suboptimal maturation after Mtb infection, impairing T cell activation, and contributing to TB susceptibility.

Introduction

TOLLIP is a master regulator of innate immune function. In genetic studies, decreased TOLLIP expression is associated with increased tuberculosis (TB) risk(1, 2). A functional promoter-region single-nucleotide polymorphism (SNP), rs5743854 G allele, contributes to decreased TOLLIP expression in monocytes (3, 4). TOLLIP deficiency is associated with decreased BCG-specific IL-2+CD4+ T-cell frequency in South African infants(1). Bacille Calmette-Guerin (BCG) is the only currently approved vaccine for TB provided to millions

[#]Correspondence: Javeed A. Shah, jashah@uw.edu; Ph: 206-543-8728; F: 206-339-1771.

of infants annually, but its effectiveness is partial and variable(5). Therefore, understanding factors that determine vaccine-induced immune factors may provide insight into improved vaccine design. How TOLLIP influences the induction of T cell memory responses is poorly understood.

One critical component for inducing T cell responses after BCG vaccination are dendritic cells (DC), which are professional antigen presenting cells essential for host immunity to *Mycobacterium tuberculosis*. In mice, DC depletion during Mtb infection leads to impaired CD4+ T cell responses and worsened disease (6). Individuals with MonoMAC syndrome, a rare genetic disorder, exhibit few DC overall and develop disseminated mycobacterial diseases early in life (7). Mtb restricts DC function in the lung by delaying antigen uptake and migration (8), and techniques to stimulate DC function during Mtb infection can reduce Mtb severity (9). Therefore, optimizing DC and T cell interactions during Mtb infection may be an effective prevention or therapeutic strategy.

Although the function of TOLLIP in DCs is unknown, TOLLIP influences the activity of multiple functionally distinct immune cell subsets. In macrophages, TOLLIP dampens NF-κB signaling, while in fibroblasts it stabilizes STING due to its role in endosomal trafficking (10–13). TOLLIP contributes to eosinophil recruitment to the lung in asthma and impaired immune responses during rhinovirus infection (14, 15), is required for effective neutrophil infiltration of solid tumors (16), and is associated with worsened disease from the intracellular pathogens *Legionella pneumophila* and *Leishmania major* (17, 18). During prolonged Mtb infection, mice lacking *Tollip* develop worsened TB disease accompanied by impaired alveolar macrophage function(1). Taken with its known effects on T cell memory responses after BCG vaccination, the lack of understanding of its impact on DC function represents a fundamental gap in knowledge.

Common genetic variation influences the cellular innate immune response to Mtb. Genetic variation impacts innate immune cellular distribution and inflammatory ligand-induced cytokine responses in peripheral blood (19–22). These effects are often immune-cell specific, so evaluating critical immune cells of interest specifically is critical for understanding genetic regulation of immune-mediated diseases (23). Therefore, we used a validated whole-blood innate immune assay to assess the influence of SNP rs5743854 on TOLLIP mRNA expression and TLR-induced cytokine responses in DCs. We followed these studies with evaluation of DC function in knockout mouse models to understand the impact on TB disease and BCG-induced T cell responses (24, 25).

Materials and Methods

Study Participants and Ethics Statement

Approval for all human study protocols was obtained from the institutional review boards at the University of Washington. Written informed consent was obtained from all participants before inclusion in the study. All participants were healthy adults >18 years of age, not taking any immunomodulatory medications, and without any medical history of cancer, kidney disease, liver disease, or recurrent or serious infections. Study participants were local volunteers self-described as healthy without history of recurrent or serious infections.

We collected peripheral whole blood from two cohorts of study volunteers to perform our genetic analysis -- one set stimulated for 6 hours and second for 24 hours. Baseline demographic characteristics of these cohorts are described in Table 1. Genotypes were determined with a Taqman genotyping assay and a Fluidigm Biomark HD 96.96 array platform or a single assay format with RTPCR and intermittently validated by sequencing of the TOLLIP promoter region.

Reagents

RPMI Medium 1640 and DMEM were purchased from Invitrogen (Carlsbad, CA.). Fetal bovine serum was purchased from Atlas Biologicals (Fort Collins, CO). Ultrapure LPS was purified from Sal*monella minnesota* R595 (List Biological Laboratories). Recombinant human and mouse cytokines (IL-4, GM-CSF) were purchased from Peprotech. Tetramers were obtained from the NIH Tetramer Core Facility

Human Peripheral Blood Assays and Flow Cytometry

For human studies, whole blood from healthy volunteers was collected in heparinized tubes and stimulated with media or LPS (10ng/ml) immediately after collection. Brefeldin A and monensin were added 4 hours prior to the end of the assay. Samples were placed in 40% RPMI media, 40% DMSO, and 10%FCS, then slowly frozen in isopropanol container followed by transfer to liquid nitrogen. These samples were thawed in batches at the time of data analysis. Flow cytometry was performed at the University of Washington Center for Emerging and Reemerging Infectious Diseases Clinical Research Facility on a BD Fortessa 5-laser flow cytometer or on BD Symphony flow cytometer. The following antibodies were used in these experiments: anti-CD3 PE-Texas Red (clone UCHT1; Beckman Coulter), anti-CD11c APC (clone 5-HCL-3; BD), anti-CD14 V500 (clone M5E2; BD), anti-CD16 (clone 3G8; Biolegend), anti-CD66 -biotin (clone ASL-32; Biolegend), anti-CD123 PE-Cy7 (clone 6H6; Biolegend), anti-HLA-DR (clone LN3; eBioscience), anti-IL-6 (clone MQ213A5; eBioscience), anti-IL12 eFluor450 (clone C8.6; eBioscience), Streptavidin V786 (BD), anti-TNF AlexaFluor-700 (clone Mab11, BD). Gating was performed manually, and cytokine responses were defined using preselected positive and negative control samples, then generalized across the entire population. Genomic DNA was obtained from PBMC using peripheral blood DNA collection kits (Qiagen, Inc). Human peripheral blood DC were prepared by isolating PBMC from peripheral blood via Ficoll gradient separation. Monocytes were then isolated via CD14+ selection using Miltenyi CD14-Human Microbead Kits. Bone marrow and resuspended in RPMI media supplemented with 10% FCS, and cells were differentiated in the presence of recombinant human GM-CSF (300 IU/ml) and IL-4 (200 IU/ml; Peprotech, Inc.) for five days. Cells in suspension were confirmed to be DC by CD14 and CD11c cell surface marker staining (>90% purity). RNA was extracted from monocyte-derived DC in cell culture using RNeasy kits (Qiagen, Inc).

Western blots

DC extracts were prepared in RIPA buffer and equal amounts of total protein (5 or 20μg), as quantified by Pierec® BCA assay (Thermo Scientific) were separated by SDS-PAGE, transferred onto nitrocellulose membranes and exposed overnight with primary antibodies to TOLLIP (Abcam, Inc) or b-actin (Cell Signaling Technologies) in TBS-T

buffer supplemented with 5% BSA. HRP-conjugated anti-rabbit IgG and SignalFire or SignalFire Elite ECL reagents (Cell Signaling Technologies) were sequentially added to membranes and densitometry was performed using a C-DiGit scanner with Image Studio 4.0 software (LiCOR).

Mice

All mice were housed and maintained in specific pathogen-free conditions at the University of Washington and Seattle Children's Research Institute, and all experiments were performed in compliance with US DHHS guidance for the care and use of laboratory animals, under the supervision of the Institutional Animal Care and Use Committee from the University of Washington and Seattle Children's Research Institute. B6.Cg-Tolliptm1$^{Kbns/Cnrm}$ (*Tollip*$^{-/-}$) mice were obtained from the European Mutant Mouse Archive (www.infrafrontier.eu) (10). Mice were backcrossed 11 times on C57BL/6J background and were confirmed to be >99% C57BL/6J genetically by screening 150 SNP ancestry informative markers (Jax, Inc). Genotyping was performed using DNA primers for neomycin (Forward sequence: AGG ATC TCC TGT CAT CTC ACC TTG CTC CTG; Reverse sequence AAG AAC TCG TCA AGA AGG CGA TAG AAG GCG) and the first exon of TOLLIP (Forward sequence: AGC TAC TGG GAG GCC ATA CA; Reverse sequence: CGT GTA CGG GAG ACC CAT TT). Protein expression was confirmed in both knockout and backcrossed alleles by Western blot selectively. All wild type control mice were age- and sex-matched littermates to ensure a common genetic background. Mice used in the experiments were 6–12 weeks of age. ABSL3 experiments were performed at the Seattle Children's Global Infectious Disease Research Institute.

Mtb infection

Aerosol infections were performed with Mtb H37Rv strain with an mCherry reporter plasmid. Mice were enclosed in a Glas-Col aerosol infection chamber and ~50–100 CFU were deposited into mouse lungs. Doses were confirmed using control mice by plating lung homogenates on 7H10 agar immediately after aerosol infection.

Tissue Preparation and Evaluation

Mice were euthanized and lungs were gently homogenized in HEPES buffer containing Liberase Blendzyme 3 (70 μg/ml; Roche) and DNaseI (30 μg/ml; Sigma-Aldrich) using a gentleMacs dissociator (Miltenyi Biotec). The lungs were then incubated for 30 min at 37°C and then further homogenized a second time with the gentleMacs. The homogenates were filtered through a 70 μm cell strainer, pelleted for RBC lysis with RBC lysing buffer (Thermo), and resuspended in FACS buffer (PBS containing 2.5% FBS and 0.1% NaN_3).

Chimera Generation

WT:*Tollip*$^{-/-}$ mixed bone marrow chimeras were generated in the following manner: WT B6.SJL-Ptprca Pepcb/BoyJ (CD45.1+; Jax, Inc.) F1 mice were lethally irradiated (1000 cGy). A 1:1 mixture of CD3-depleted (Miltenyi Biotec) *Tollip*$^{-/-}$ (CD45.2+) and F1 generation of C57BL/6J (CD45.1+45.2+) bone marrow was provided intravenously. Mice were allowed to recover for at least ten weeks before experiments were performed.

Cellular Assays

Bone marrow was harvested from mice and grown in RPMI supplemented with 10% heat inactivated FCS (Atlas Bio, Fort Collins, CO). Bone marrow-derived dendritic cells (BMDC) were differentiated in the presence of IL-4 and GM-CSF (Peprotech, Inc.) for 7 days (26). For T cell coculture experiments, naïve CD4 T cells were isolated using magnetic bead-conjugated antibodies (EasySep™ Murine CD4+ T Cell Isolation Kit) from homogenized splenocytes, stained with CFSE at 37° C for 15 minutes, and washed three times with PBS. T cells were added to BMDC-containing wells at a density of 200,000 cells/well and media was supplemented with 10ng/mL IL-2 at day 2 and 3. Following differentiation, BMDCs were plated with OVA323–330 peptide (10μg/ml) for 2 hours, then OVA-specific CD4+ T cells were added at 1:10 BMDC:T cell ratio. Cells were harvested after 7 days and analyzed via flow cytometry. Cytokine concentrations from cellular supernatants were performed by ELISA (R&D Biosystems, ELISA Duosets).

Mouse Flow Cytometry

Lung single cell suspensions were washed and stained for viability with Zombie Aqua viability dye (BioLegend) for 10 min at room temperature in the dark. After incubation, 100μl of a surface antibody cocktail diluted in 50% FACS buffer/50% 24G2 Fc blocking buffer was added, and surface staining was performed for 30 min at 4°C. Cells were washed once with FACS buffer and fixed with 2% paraformaldehyde for 1 h prior to analyzing on an LSRII flow cytometer (BD Biosciences). In some experiments, intracellular staining was performed after surface staining. Permeabilization was performed with Fix-Perm buffer (eBiosciences) for minimum of 60 min before the addition of intracellular antibodies. The following antibodies were used for these experiments: anti-CD80 (Invitrogen, cat: 11-0801-85), anti-CD40 (Biolegend cat: 124624), anti-CD11b (BD cat: 562681and Biolegend cat: 101243), Zombie Aqua viability (Biolegend, cat: 423102), anti-Ly6G (Biolegend cat: 127614 and BD cat: 561105), MHC Class II (I-A/I-E; Biolegend cat: 107622 and Biolegend cat: 107620), anti-CD11c (Biolegend cat: 117339), anti-CD103 (BD cat: 564322), anti-CD45.2 (Biolegend cat: 109828 and Biolegend cat: 109814), anti-CD45.1 (Invitrogen cat: A14733). Some mouse flow experiments were performed on a BD Symphony A3 flow cytometer at the University of Washington Flow Cytometry Core Facility and others were performed on a BD FacsLSR II at Seattle Children’s’ Research Institute.

Statistical methods

Statistical association between SNP rs5743854 and cytokine-induced phenotypes were determined using a simple generalized linear model comparing genotypes (AA vs Aa vs aa). Because SNP rs5743854 has been validated as functionally active, we used a p-value threshold of < 0.05 to determine statistical significance, without correction for multiple comparisons. For mouse studies, comparisons were made with two-sided t tests unless otherwise described. A p-value threshold of <0.05 was used to determine statistical significance. Statistical analysis and visualizations of data were performed with Prism version 8.0 (GraphPad, Inc.).

Results

SNP rs5743854 is associated with decreased mRNA expression in DCs

In prior studies, the G allele of rs5743854 was associated with decreased frequency of BCG-specific IL-2+CD4+ T cells (2). This variant was associated with TOLLIP expression in monocytes, so we first evaluated DCs, as a related cell type with a primary role in inducing and maintaining T cell responses (27, 28). We used a genetic approach to evaluate the impact of TOLLIP on human DC function. We differentiated DC from peripheral blood monocytes then extracted RNA and measured *TOLLIP* mRNA expression (29). SNP rs5743854 G allele was associated with diminished *TOLLIP* mRNA expression (Figure 1A; $p = 0.03$, generalized linear model). Further, rs5743854 G allele was associated with TOLLIP protein expression in BMDC by Western blot (Figure 1B–C; $p < 0.04$, two-sided t-test). Therefore, SNP rs5743854 is broadly associated with diminished mRNA expression and protein expression in BMDC, making it a useful tool to study the effects of TOLLIP in DC in human populations.

SNP rs5743854 is associated with diminished LPS-induced IL-12 in peripheral blood DC

Based on these results, we measured the association between rs5743854 and the proportion of peripheral blood HLA-DR+CD11c+ DC, CD123+ plasmacytoid DC (pDC), or CD14+ monocytes producing IL-12, TNF, or IL-6, after six hours of media or LPS stimulation (Figure 2A) by intracellular cytokine staining (gating in Figure S1)(30, 31). In CD11c+ DC, the G allele of SNP rs5743854 was associated with decreased IL-12 (Figure 2B; $p = 0.003$, generalized linear model) and TNF (Figure 2C; $p = 0.02$), but not IL-6 (Figure 2D). In pDC, overall cytokine responses were low, and rs5743854 was not associated with IL-12, IL-6, or TNF expression (data not shown). In prior studies using cultured monocytes, rs5743854 G allele was associated with increased IL-6 and TNF by ELISA (2). We compared our findings in DC with CD14+ monocytes to provide direct comparisons across cell types. We did not find significant association between rs5743854 and IL-12 in CD14+ monocytes, (Figure 2E) but rs5743854 was associated with increased TNF in monocytes (Figure 2F, $p = 0.001$) and a trend toward increased IL-6, although this did not achieve statistical significance (Figure 2G).

As part of an evaluation of LPS-induced cytokine responses in the whole blood of healthy volunteers, samples were stimulated for both 6hr and 24hr to better define maximal ranges of different cytokines with different response kinetics. Although the timing of the responses was different, we used this study to validate findings made in the initial cohort, an important component for reproducibility in genetic studies (Figure 2H). Again, the G allele of SNP rs5743854 was associated with diminished IL-12 (Figure 2I; $p = 0.03$). We did not detect significant association between rs5743854 and TNF or IL-6 (Figure 2J–K). In CD14+ monocytes, SNP rs5743854 G allele was not associated with IL-12 (Figure 2L), but was associated with increased TNF (Figure 2M, $p = 0.049$), but not IL-6 (Figure 2N). Overall, we found a strong association between rs5743854 G allele and diminished IL-12 in CD11c+ DC, but increased TNF from LPS-stimulated monocytes. These data suggest that TOLLIP has divergent effects on DCs and monocytes after LPS stimulation (3).

Tollip$^{-/-}$ DC develop diminished maturation *in vitro*

We next evaluated DC function in *Tollip*$^{-/-}$ mice to validate our genetic observations in an alternate model of TOLLIP deficiency and to understand the impact of TOLLIP on lung and lymph node-resident DC maturation during live Mtb infection. We incubated IL-4/GM-CSF-differentiated bone marrow-derived DC (BMDC) with LPS (10ng/ml) overnight and measured IL-12p70, TNF, and IL-10 concentrations from the cellular supernatants. *Tollip*$^{-/-}$ BMDC secreted significantly less IL-12 (Figure 3A; p=0.04) and TNF (Figure 3B; p=0.0001), but more IL-10 (Figure 3C; p = 0.01). We also differentiated bone marrow in Flt3L for seven days to induce an alternate DC phenotype and measured IL-12p70, TNF, and IL-10 after LPS stimulation (32). Although these cells did not produce IL-12, we found diminished TNF (Figure 3D, p=0.0001), and increased IL-10 (Figure 3E, p = 0.03) in *Tollip*$^{-/-}$ mice. Because these responses may be distinct to DC, we also measured cytokine responses in bone marrow-derived macrophages (BMDM), isolated from WT and *Tollip*$^{-/-}$ mice, after LPS stimulation. IL-12p70 secretion was unaffected by TOLLIP (Figure 3D), but TNF was increased in *Tollip*$^{-/-}$ BMDM (Figure 3E, p = 0.0002), and IL-10 was diminished (Figure 3F, p = 0.001). After observing that TOLLIP potentiated IL-12p70 production in DCs, we tested the role of TOLLIP on MHC Class II and CD40 cell surface expression. *Tollip*$^{-/-}$ BMDC only partially increased CD40 expression in response to LPS maturation (Figure 3G–H, p=0.03), but MHC Class II expression was normal in *Tollip*$^{-/-}$ BMDC (Figure 3I). Therefore, TOLLIP significantly contributes to DC maturation.

Tollip$^{-/-}$ DC demonstrate impaired maturation in Mtb-infected lungs and lymph nodes

Because DCs are essential for Mtb control in both mice and human populations, we examined the role of TOLLIP on DC function during pulmonary Mtb infection. We infected B6 and *Tollip*$^{-/-}$ mice with 50 CFU of Mtb-H37Rv expressing a fluorescent mCherry reporter (Mtb-mCherry). After 28 days, we isolated lung tissue and generated single cell suspensions to identify and characterize lung-resident DC populations by flow cytometry. The proportion of overall CD11c+ DC was similar between WT and *Tollip*$^{-/-}$ mice after 28 days of infection, suggesting no alteration in DC development in mice lacking *Tollip* (Figure 4A). Within the DC compartment, we identified two DC populations in the lungs of Mtb infected mice: (MHCII+CD11c+SiglecF-Ly6G-CD11b+CD103- (CD11b+ DC) and MHCII+CD11c+SiglecF-Ly6G-CD11b-CD103+ DC (CD103+ DC; representative gating, Figure S2A). Basal numbers and expression of MHC-II, CD40, and CD80 were similar in splenic CD11c+ DC from healthy eight week old B6 and *Tollip*$^{-/-}$ mice (Figure S2B). We measured costimulatory marker expression in these cells as a proxy for overall DC maturation. We measured CD80 expression, a canonical cell surface expression marker which is induced during DC maturation(33). CD80 expression on *Tollip*$^{-/-}$ CD11b+ DC was significantly diminished (Figure 4B; p = 0.048). Similarly, CD80 expression on CD103+ DCs was also decreased but did not achieve statistical significance (Figure 4C; p = 0.056). MHC Class II expression was significantly decreased in *Tollip*$^{-/-}$ CD11b+ DC (Figure 4D; p = 0.002) and CD103+ DC (Figure 4E; p = 0.02). These data suggest that defects in *Tollip*$^{-/-}$ DC maturation were similar in both CD11b+ DC and CD103+ DC, and they are present within Mtb-infected lung tissue.

Tollip intrinsically impairs lung-resident DC function in Mtb-infected mice

Based on our observations that DC from *Tollip*$^{-/-}$ mice are abnormal during Mtb infection, we evaluated the intrinsic effects of TOLLIP on DC using mixed bone marrow chimeric mice, a model that permits evaluation of the DC-intrinsic function of TOLLIP, independently from the effects of cell-cell interactions, environmental effects, or bacterial burden. We lethally irradiated B6.SJL-Ptprc^{a} Pepc^{b}/BoyJ mice (CD45.1+), which express the differential CD45.1 pan-leukocyte marker, then administered 5×10^{6} bone marrow cells, composed of a 1:1 mix of CD45.1+ *Tollip*$^{+/+}$ and CD45.2+ *Tollip*$^{-/-}$ cells. After waiting 10 weeks for immune reconstitution, we infected chimeras with 50 CFU of Mtb-mCherry and measured DC phenotypes 14, 16, 19, 21, and 28 days after infection. Our primary goal was to characterize the intrinsic role of TOLLIP on cell surface markers of DC maturation MHC-II and CD40 longitudinally during the early stages of Mtb infection (Figure 5A; gating strategy, Figure S3A). As in whole-body knockout mice, basal expression of MHC-II, CD40, and CD80 were no different between B6 and *Tollip*$^{-/-}$ lineages in mixed bone marrow chimeric mice at baseline (Figure S3B). Mixed bone marrow mice had similar proportions of CD45.1/2+ (WT) and CD45.2+ (*Tollip*$^{-/-}$) cells (Figure 5B). In the lungs, *Tollip*$^{-/-}$ CD11b+ DC demonstrated diminished CD40 expression at every time point measured (Figure 5C). By contrast, MHC-II expression was diminished in *Tollip*$^{-/-}$ CD11b+ DC 14 days after infection, but then progressively normalized (Figure 5D). These data suggest that TOLLIP contributes significantly to CD40 upregulation *in vivo*, but that defects in MHC Class II expression are temporary during prolonged Mtb infection.

During Mtb infection, the bulk of T cell priming occurs in the draining mediastinal lymph nodes (MLN)(34, 35). Therefore, we measured the cell surface expression of MHC Class II and CD40 from DC mixed bone marrow chimeric mice in MLN tissue. 19 and 21, but not 28 days after infection, *Tollip*$^{-/-}$ DC had diminished CD40 cell surface expression (Figure 5E). MHC-II expression was diminished 21 days post infection, but not at other time points (Figure 5F). Therefore, costimulatory marker expression in *Tollip*$^{-/-}$ DC was impaired in lung, and to a lesser extent MLN, during Mtb infection, while TOLLIP delayed MHC-II upregulation. *Tollip*$^{-/-}$ DC located in tissue compartments critical for T cell activation during Mtb infection demonstrate impaired maturation after Mtb infection.

Tollip$^{-/-}$ mice develop diminished T cell responses after Mtb infection and BCG vaccination

We measured the frequency of Mtb-specific T cells in *Tollip*$^{-/-}$ mice (36) with MHC-II tetramers recognizing the immunodominant ESAT-6 epitope (37–40) 28 days after aerosol Mtb infection (50 CFU) (gating strategy; Figure S4B) in the lungs and mediastinal lymph nodes (MLN). Day 28–34 after Mtb infection generally represents the peak of the CD4+ T cell response in B6 mice (40). We observed fewer ESAT-6-specific CD4+ T cells in the lungs of *Tollip*$^{-/-}$ mice (Figure 6A, representative image, Figure 6B)(41). These data suggest that TOLLIP is required for maximal antigen-specific CD4+ T cell responses during Mtb infection.

Although Mtb-specific T cell responses were diminished, these may be due to altered Mtb burden at the time point selected. To address this issue and extend our observations in

an alternate mycobacteria, we evaluated TOLLIP's effect on BCG vaccine-specific T cell responses. Understanding the role of TOLLIP on BCG, the vaccine provided to infants for over 100 years, may provide insight into potential roles for TOLLIP on vaccine induced immunity and protection as well as Mtb pathogenesis (42). We vaccinated B6 and *Tollip*$^{-/-}$ mice with 10^6 CFU BCG (Russia strain, gift of David Sherman) via the intravenous method (IV BCG), a strategy which strongly induces antigen-specific T cell responses and controls Mtb infection in non-human primates (43). Eight weeks after vaccination, we measured systemic BCG-specific CD4+ and CD8+ T cell responses in the spleen by restimulation with overlapping pooled peptides of mycobacterial Antigen 85A and 85B (Ag85A/B) for six hours (gating in Figure S4B), followed by measuring the frequency of BCG-specific IL-2, TNF, and IFNγ in CD4+ cells by intracellular cytokine staining. BCG bacterial CFU were similar in the spleens of B6 and *Tollip*$^{-/-}$ mice four weeks after vaccination (Figure S4C). IV BCG in B6 mice induced strong increases in the proportion of CD4+ T cells producing IL-2 (Figure 7A; $p < 0.0001$), TNF (Figure 7B; $p = 0.02$), and IFNγ (Figure 7C; $p < 0.0001$), but few cytokine-producing CD4+ cells from BCG-vaccinated, *Tollip*$^{-/-}$ mice were detectable. Therefore, TOLLIP assists in priming and maintaining CD4+ T cell memory to Mtb infection and BCG vaccination.

TOLLIP is critical role for BCG-induced T cell responses, but T cell priming is influenced by several factors, including antigenic burden and T cell factors (44, 45). To further evaluate the role of TOLLIP on its importance for DCs function on T cell priming, we used a coculture model to determine the capacity of *Tollip*$^{-/-}$ DCs to activate T cell proliferation. We cultured CFSE-labeled CD4+ T cells isolated from B6.Cg-Tg(TcraTcrb)425Cbn/J (OT-II) mice, whose transgenic CD4+ T cells primarily recognize the chicken ovalbumin 323–339 peptide (OVA), with WT and *Tollip*$^{-/-}$ BMDC, pulsed with OVA or BSA as a control, and measured cellular division after seven days. *Tollip*$^{-/-}$ BMDC, compared to WT BMDC, did not promote T cell proliferation optimally (Figure 7D–E). Therefore, *Tollip*$^{-/-}$ DC demonstrate diminished functional capacity to stimulate T cell responses and demonstrate a significant role for TOLLIP in DC priming of T cells.

Discussion

Our data suggests that TOLLIP plays a critical role in maintaining DC function in peripheral blood, lymph node, and lung, in both mice and humans, and this contributes to the effective development of vaccine-induced CD4+ T cell responses.

TOLLIP deficiency was associated with divergent phenotypes between DC and monocytes. *Tollip*$^{-/-}$ macrophages produced increased TNF, but decreased IL-10 in response to LPS, but LPS-stimulated, *Tollip*$^{-/-}$ DC produced less IL-12 and TNF, and increased IL-10. To our knowledge, few other genes are responsible for divergent phenotypes between different cells of the same myeloid lineage after inflammatory activation. However, proteins in the autophagy pathway, which includes TOLLIP, influence macrophage and DC function differentially, TOLLIP is an autophagy adaptor protein acting downstream from master autophagy switches mTOR and Beclin-1 (46). Based on this similar potential pathway of action, its effects should mimic those of beclin-1 on innate immune responses. Decreased beclin-1 expression is associated with decreased frequency of antigen-specific IFN-γ+

CD4+T cells and impaired DC function during respiratory syncytial virus infection, which suggests diminished IL-12 secretion in these DC (47). By contrast, beclin-1 haploinsufficiency in macrophages leads to increased TNF and IL-6 secretion after TLR4 activation and worsens inflammation in experimental colitis (48). These data mirror the responses we detected in our TOLLIP-deficiency models and suggest that TOLLIP contributes similarly to regulation of innate immunity. The fact that TOLLIP is responsible for some or all of beclin-1's effects on innate immune responses make it an attractive target for therapeutic modulation, as it may induce strong immune changes with fewer adverse off-target effects that limit the therapeutic potential of other autophagy modulators (49). Understanding how TOLLIP influences host immune responses may lead to better therapeutics to shape the immune response.

TOLLIP has divergent roles across multiple immune cell types. In this study, we found that TOLLIP influences DC immune function. In other studies, we found that TOLLIP maintains cellular homeostasis in macrophages by controlling lipid accumulation via the EIF2-induced cellular stress response, in addition to influencing macrophage immune responses (36). These studies suggest that TOLLIP's cellular functions are context-dependent. TOLLIP transports diverse cargo, including lipids, protein aggregates, mitochondria, immune receptors STING and IL-1R, and others(10, 13, 50, 51). Under different environmental conditions, its lipid and protein scavenging function competes with immune receptors for TOLLIP binding, thus altering its apparent function. TOLLIP stabilizes the immune receptor STING, but protein degradation within the endoplasmic reticulum directly competes with this effect(13). Therefore, specific cellular conditions, including the variety of immune receptors and signaling kinases, the amount of lipid and protein requiring degradation, and cellular environment influence TOLLIP's cargo and alter cellular function distinctly across multiple immune cell types. Understanding the intracellular factors that contribute to TOLLIP's function in distinct cell types may elucidate how environmental factors may influence immune function.

How TOLLIP influences antigen presentation is not well understood. Both MHC Class I and MHC Class II are assembled and transported to the cell surface in the endoplasmic reticulum (ER) (52). In macrophages, TOLLIP diminishes cell surface expression of TLR2, TLR4, and IL-1R via endosomal transport from the cell surface to lysosomes (10, 53, 54). TOLLIP clears misfolded proteins and lipids from the ER and contributes to maintaining effective ER activity (1, 13). TOLLIP binds to MARCH1, a ubiquitin ligase that modifies MHC Class II and supports its expression on the cell surface (55). These data suggest that TOLLIP contributes to the assembly and delivery of critical antigen presentation products, as well as transport of cell surface markers from the ER to the cell surface. Understanding the complex interplay between cell surface cargo and endosomal transport protein may provide insight into immune regulation.

CD40 expression in *Tollip*$^{-/-}$ DC from mixed chimeric mice was diminished for at least 28 days, but CD40 and MHC-II expression normalized in the MLN between 21 and 28 days after infection. These data suggest that lung-resident DC maturation are more dependent on *Tollip* than MLN-resident DC after Mtb infection. Immune responses at the site of granulomas are quite different from systemic responses (56, 57). A major difference

between lungs and LN during Mtb infection is that the granuloma is created in the setting of significant compromise to the environmental conditions within the lung. Mtb-infected lungs display low oxygen tension and amino acide availability with high lipid concentrations. These conditions are suboptimal for immune activation and function (58, 59). By contrast, the environment within MLN are generally optimized, both in structure and nutrient content, to facilitate immune crosstalk (60). In global transcriptional analysis of human granulomas, *TOLLIP* mRNA was increased within TB granulomas, but not in peripheral blood (1, 61). In Mtb-infected alveolar macrophages, *Tollip* deletion induces the integrated stress response, which coordinates cellular adaptation to variable environmental conditions (1). These changes, which include alterations in cell division, energetics, and survival, may impair DC maturation and optimal antigen presentation (62, 63). Understanding the specific mechanisms by which TOLLIP influences DC responses within the lung may lead to novel strategies to improve Mtb control within granulomas.

We recognize limitations in our study. The genetic association we identified may be due to effects beyond TOLLIP due to linkage disequilibrium with nearby genes. However, rs5743854 is functional in the promoter region and we validated that this SNP was associated with diminished TOLLIP mRNA expression in DC as well as monocytes (2). We were unable to directly measure TOLLIP expression in peripheral blood DC. However, we found differences in TOLLIP mRNA and protein expression in monocyte-derived dendritic cells. We combined these observations with differences in cytokine responses in peripheral blood DC, and lung-resident function in $Tollip^{-/-}$ DC was altered as well, providing orthogonal support for our observations that TOLLIP variation influences DC activity. In our mouse studies, T cell priming during Mtb infection involves DC migration. DC are infected by Mtb in the lung, then undergo transport to MLN. However, much of the priming in this tissue space is accomplished by resident DCs and other myeloid cells in the LN (8, 64). TOLLIP is important for DC function in both tissue compartments, but we did not evaluate the effect of TOLLIP on DC migration itself. CD40 expression and ligation are associated with DC migration, so we presume that $Tollip^{-/-}$ DC will have impaired migration as well (65). Although we did not note significant overall differences in MHC-II expression in $Tollip^{-/-}$ DC in the LN in our mixed bone marrow chimeric mice, we found a diminished proportion of MHC-II-high DC, which may be a marker for migratory DC and suggest a role for TOLLIP in DC migration during Mtb infection. BCG-specific T cell responses in our B6 mouse model were somewhat diminished compared to expected results, based on the published literature. Although much of this result can be explained by nonspecific activation in control mice, our laboratory-grown BCG may be somewhat less immunogenic than commercial strains. Non-tuberculous mycobacteria from water may influence the basal responses to BCG (66). Despite this relative decrease, we found that T cell responses to both Mtb and BCG were diminished, demonstrating a robust influence of TOLLIP on T cell responses to mycobacteria. Future studies will directly address this issue and its significance on Mtb outcomes.

TOLLIP was required for the formation of memory T cell responses. Although we focused on the role of TOLLIP in DC in this study, TOLLIP may act directly upon T cells. TAX1BP1, an autophagy receptor with similar protein domains as TOLLIP, influences T cell activation by recruiting amino acids to support cell cycle activation (67). Rapamycin induces

autophagy, which dramatically changes the capacity for T cells to respond to pathogens (68). However, TOLLIP has a significant effect directly on DC priming of T cell antigens *in vitro*, suggesting an important independent contribution of DC on T cell priming. Future studies will evaluate the impact of TOLLIP on T cell activation, longevity, and death, to fully evaluate the impact of TOLLIP on the host immune response during Mtb infection. Understanding the factors that contribute to T cell migration and activation within the Mtb-infected lung are critical for vaccine development.

In conclusion, TOLLIP is essential for DC maturation and function, including proinflammatory cytokine production, surface molecule expression, and antigen presentation. Individuals with decreased TOLLIP expression have diminished DC function and BCG-specific T cell responses, which may substantially contribute to increased risk for TB. Identifying mechanisms to selectively increase TOLLIP activity and function in DC may lead to important improvements in TB vaccine design and immune drug development.

Supplementary Material

Refer to Web version on PubMed Central for supplementary material.

Acknowledgements

The authors would like to thank the study participants for their generous interest in our work. We would also like to thank the Cell Analysis Facility Shared Resource at the University of Washington for use of their flow cytometers and technical resources. We would also like to thank Chetan Seshadri and Erik Layton for helpful technical conversations.

Grant Support; P01 AI 132130 to TRH and JAS; R01 AI136921 to JAS; 1S10OD024979.

References

1. Venkatasubramanian S, Plumlee C, Dill-McFarland K, Pearson GL, Cohen SB, Lietzke A, Pacheco A, Hinderstein SA, Emery R, Soleimanpour SA, Altman M, Urdahl KB, and Shah JA. 2020. TOLLIP resolves lipid-induced EIF2 signaling in alveolar macrophages for durable Mycobacterium tuberculosis protection. bioRxiv.
2. Shah JA, Musvosvi M, Shey M, Horne DJ, Wells RD, Peterson GJ, Cox JS, Daya M, Hoal EG, Lin L, Gottardo R, Hanekom WA, Scriba TJ, Hatherill M, and Hawn TR. 2017. A Functional TOLLIP Variant is Associated with BCG-Specific Immune Responses and Tuberculosis. Am J Respir Crit Care Med.
3. Shah JA, Vary JC, Chau TT, Bang ND, Yen NT, Farrar JJ, Dunstan SJ, and Hawn TR. 2012. Human TOLLIP Regulates TLR2 and TLR4 Signaling and Its Polymorphisms Are Associated with Susceptibility to Tuberculosis. J Immunol 189: 1737–1746. [PubMed: 22778396]
4. Katayanagi S, Setoguchi Y, Kitagawa S, Okamoto T, and Miyazaki Y. 2021. Alternative gene expression by TOLLIP variant is associated with lung function in chronic hypersensitivity pneumonitis. Chest.
5. Ahmed A, Rakshit S, Adiga V, Dias M, Dwarkanath P, D'Souza G, and Vyakarnam A. 2021. A century of BCG: Impact on tuberculosis control and beyond. Immunol Rev 301: 98–121. [PubMed: 33955564]
6. Tian T, Woodworth J, Sköld M, and Behar SM. 2005. In Vivo Depletion of CD11c+ Cells Delays the CD4+ T Cell Response to Mycobacterium tuberculosis and Exacerbates the Outcome of Infection. The Journal of Immunology 175: 3268–3272. [PubMed: 16116218]

7. Camargo JF, Lobo SA, Hsu AP, Zerbe CS, Wormser GP, and Holland SM. 2013. MonoMAC syndrome in a patient with a GATA2 mutation: case report and review of the literature. Clin Infect Dis 57: 697–699. [PubMed: 23728141]
8. Wolf AJ, Linas B, Trevejo-Nuñez GJ, Kincaid E, Tamura T, Takatsu K, and Ernst JD. 2007. Mycobacterium tuberculosis infects dendritic cells with high frequency and impairs their function in vivo. In Journal of immunology (Baltimore, Md : 1950). 2509–2519.
9. Griffiths KL, Ahmed M, Das S, Gopal R, Horne W, Connell TD, Moynihan KD, Kolls JK, Irvine DJ, Artyomov MN, Rangel-Moreno J, and Khader SA. 2016. Targeting dendritic cells to accelerate T-cell activation overcomes a bottleneck in tuberculosis vaccine efficacy. Nature communications 7: 13894.
10. Burns K, Clatworthy J, Martin L, Martinon F, Plumpton C, Maschera B, Lewis A, Ray K, Tschopp J, and Volpe F. 2000. Tollip, a new component of the IL-1RI pathway, links IRAK to the IL-1 receptor. Nat Cell Biol 2: 346–351. [PubMed: 10854325]
11. Bulut Y, Faure E, Thomas L, Equils O, and Arditi M. 2001. Cooperation of Toll-like receptor 2 and 6 for cellular activation by soluble tuberculosis factor and Borrelia burgdorferi outer surface protein A lipoprotein: role of Toll-interacting protein and IL-1 receptor signaling molecules in Toll-like receptor 2 signaling. In J Immunol. 987–994. [PubMed: 11441107]
12. Zhang G, Ghosh S 2002. Negative Regulation of Toll-like Receptor-mediated Signaling by Tollip. Journal of Biological Chemistry 277: 7059–7065. [PubMed: 11751856]
13. Pokatayev V, Yang K, Tu X, Dobbs N, Wu J, Kalb RG, and Yan N. 2020. Homeostatic regulation of STING protein at the resting state by stabilizer TOLLIP. Nat Immunol 21: 158–167. [PubMed: 31932809]
14. Ito Y, Schaefer N, Sanchez A, Francisco D, Alam R, Martin RJ, Ledford JG, Stevenson C, Jiang D, Li L, Kraft M, and Chu HW. 2018. Toll-Interacting Protein, Tollip, Inhibits IL-13-Mediated Pulmonary Eosinophilic Inflammation in Mice. J Innate Immun 10: 106–118. [PubMed: 29393212]
15. Dakhama A, Mubarak RA, Pavelka N, Voelker D, Seibold M, Ledford JG, Kraft M, Li L, and Chu HW. 2019. Tollip Inhibits ST2 Signaling in Airway Epithelial Cells Exposed to Type 2 Cytokines and Rhinovirus. J Innate Immun: 1–13.
16. Begka C, Pattaroni C, Mooser C, Nancey S, Swiss IBDCSG, McCoy KD, Velin D, and Maillard MH. 2020. Toll-Interacting Protein Regulates Immune Cell Infiltration and Promotes Colitis-Associated Cancer. iScience 23: 100891. [PubMed: 32114379]
17. Parmar N, Chandrakar P, Vishwakarma P, Singh K, Mitra K, and Kar S. 2018. Leishmania donovani Exploits Tollip, a Multitasking Protein, To Impair TLR/IL-1R Signaling for Its Survival in the Host. J Immunol 201: 957–970. [PubMed: 29907707]
18. Shah JA, Emery R, Lee B, Venkatasubramanian S, Simmons JD, Brown M, Hung CF, Prins JM, Verbon A, Hawn TR, and Skerrett SJ. 2019. TOLLIP deficiency is associated with increased resistance to Legionella pneumophila pneumonia. Mucosal Immunol 12: 1382–1390. [PubMed: 31462698]
19. Li Y, Oosting M, Smeekens SP, Jaeger M, Aguirre-Gamboa R, Le KTT, Deelen P, Ricano-Ponce I, Schoffelen T, Jansen AFM, Swertz MA, Withoff S, van de Vosse E, van Deuren M, van de Veerdonk F, Zhernakova A, van der Meer JWM, Xavier RJ, Franke L, Joosten LAB, Wijmenga C, Kumar V, and Netea MG. 2016. A Functional Genomics Approach to Understand Variation in Cytokine Production in Humans. Cell 167: 1099–1110 e1014. [PubMed: 27814507]
20. Lee MN, Ye C, Villani AC, Raj T, Li W, Eisenhaure TM, Imboywa SH, Chipendo PI, Ran FA, Slowikowski K, Ward LD, Raddassi K, McCabe C, Lee MH, Frohlich IY, Hafler DA, Kellis M, Raychaudhuri S, Zhang F, Stranger BE, Benoist CO, De Jager PL, Regev A, and Hacohen N. 2014. Common genetic variants modulate pathogen-sensing responses in human dendritic cells. Science 343: 1246980. [PubMed: 24604203]
21. Roederer M, Quaye L, Mangino M, Beddall MH, Mahnke Y, Chattopadhyay P, Tosi I, Napolitano L, Terranova Barberio M, Menni C, Villanova F, Di Meglio P, Spector TD, and Nestle FO. 2015. The genetic architecture of the human immune system: a bioresource for autoimmunity and disease pathogenesis. Cell 161: 387–403. [PubMed: 25772697]

22. Barreiro LB, Tailleux L, Pai AA, Gicquel B, Marioni JC, and Gilad Y. 2012. Deciphering the genetic architecture of variation in the immune response to *Mycobacterium tuberculosis* infection. Proceedings of the National Academy of Sciences 109: 1204.

23. Schmiedel BJ, Singh D, Madrigal A, Valdovino-Gonzalez AG, White BM, Zapardiel-Gonzalo J, Ha B, Altay G, Greenbaum JA, McVicker G, Seumois G, Rao A, Kronenberg M, Peters B, and Vijayanand P. 2018. Impact of Genetic Polymorphisms on Human Immune Cell Gene Expression. Cell 175: 1701–1715 e1716. [PubMed: 30449622]

24. Shey MS, Nemes E, Whatney W, de Kock M, Africa H, Barnard C, van Rooyen M, Stone L, Riou C, Kollmann T, Hawn TR, Scriba TJ, and Hanekom WA. 2014. Maturation of innate responses to mycobacteria over the first nine months of life. J Immunol 192: 4833–4843. [PubMed: 24733845]

25. Smolen KK, Cai B, Gelinas L, Fortuno ES 3rd, Larsen M, Speert DP, Chamekh M, Cooper PJ, Esser M, Marchant A, and Kollmann TR. 2014. Single-cell analysis of innate cytokine responses to pattern recognition receptor stimulation in children across four continents. J Immunol 193: 3003–3012. [PubMed: 25135829]

26. Sallusto F, and Lanzavecchia A. 1994. Efficient presentation of soluble antigen by cultured human dendritic cells is maintained by granulocyte/macrophage colony-stimulating factor plus interleukin 4 and downregulated by tumor necrosis factor alpha. The Journal of experimental medicine 179: 1109–1118. [PubMed: 8145033]

27. Wolf AA, Yáñez A, Barman PK, and Goodridge HS. 2019. The Ontogeny of Monocyte Subsets. Front Immunol 10: 1642. [PubMed: 31379841]

28. Manz MG, Miyamoto T, Akashi K, and Weissman IL. 2002. Prospective isolation of human clonogenic common myeloid progenitors. Proceedings of the National Academy of Sciences 99: 11872–11877.

29. Schmiedel BJ, Singh D, Madrigal A, Valdovino-Gonzalez AG, White BM, Zapardiel-Gonzalo J, Ha B, Altay G, Greenbaum JA, McVicker G, Seumois G, Rao A, Kronenberg M, Peters B, and Vijayanand P. 2018. Impact of Genetic Polymorphisms on Human Immune Cell Gene Expression. Cell 175: 1701–1715.e1716. [PubMed: 30449622]

30. Kollmann TR, Crabtree J, Rein-Weston A, Blimkie D, Thommai F, Wang XY, Lavoie PM, Furlong J, Fortuno ES 3rd, Hajjar AM, Hawkins NR, Self SG, and Wilson CB. 2009. Neonatal innate TLR-mediated responses are distinct from those of adults. J Immunol 183: 7150–7160. [PubMed: 19917677]

31. Shooshtari P, Fortuno ES 3rd, Blimkie D, Yu M, Gupta A, Kollmann TR, and Brinkman RR. 2010. Correlation analysis of intracellular and secreted cytokines via the generalized integrated mean fluorescence intensity. Cytometry A 77: 873–880. [PubMed: 20629196]

32. Brasel K, De Smedt T, Smith JL, and Maliszewski CR. 2000. Generation of murine dendritic cells from flt3-ligand–supplemented bone marrow cultures. Blood, The Journal of the American Society of Hematology 96: 3029–3039.

33. Dalod M, Chelbi R, Malissen B, and Lawrence T. 2014. Dendritic cell maturation: functional specialization through signaling specificity and transcriptional programming. Embo J 33: 1104–1116. [PubMed: 24737868]

34. Srivastava S, and Ernst JD. 2014. Cell-to-cell transfer of M. tuberculosis antigens optimizes CD4 T cell priming. Cell Host Microbe 15: 741–752. [PubMed: 24922576]

35. Samstein M, Schreiber HA, Leiner IM, Susac B, Glickman MS, and Pamer EG. 2013. Essential yet limited role for CCR2(+) inflammatory monocytes during Mycobacterium tuberculosis-specific T cell priming. Elife 2: e01086. [PubMed: 24220507]

36. Sambasivan Venkatasubramanian, P. C, Dill-McFarland Kim, Pearson Gemma L., Cohen Sara B., Lietzke Anne, Pacheco Amanda, Pryor Robyn, Soleimanpour Scott A., Altman Matthew, Urdahl Kevin B., Shah Javeed A.. 2020. TOLLIP resolves lipid-induced EIF2 signaling in alveolar macrophages for durable Mycobacterium tuberculosis protection. bioRxiv.

37. Moon JJ, Chu HH, Hataye J, Pagán AJ, Pepper M, McLachlan JB, Zell T, and Jenkins MK. 2009. Tracking epitope-specific T cells. Nature Protocols 4: 565–581. [PubMed: 19373228]

38. Shafiani S, Dinh C, Ertelt JM, Moguche AO, Siddiqui I, Smigiel KS, Sharma P, Campbell DJ, Way SS, and Urdahl KB. 2013. Pathogen-specific Treg cells expand early during mycobacterium

tuberculosis infection but are later eliminated in response to Interleukin-12. Immunity 38: 1261–1270. [PubMed: 23791647]

39. Shafiani S, Tucker-Heard G, Kariyone A, Takatsu K, and Urdahl KB. 2010. Pathogen-specific regulatory T cells delay the arrival of effector T cells in the lung during early tuberculosis. J Exp Med 207: 1409–1420. [PubMed: 20547826]
40. Moguche AO, Shafiani S, Clemons C, Larson RP, Dinh C, Higdon LE, Cambier CJ, Sissons JR, Gallegos AM, Fink PJ, and Urdahl KB. 2015. ICOS and Bcl6-dependent pathways maintain a CD4 T cell population with memory-like properties during tuberculosis. The Journal of Experimental Medicine 212: 715–728. [PubMed: 25918344]
41. Reiley WW, Calayag MD, Wittmer ST, Huntington JL, Pearl JE, Fountain JJ, Martino CA, Roberts AD, Cooper AM, Winslow GM, and Woodland DL. 2008. ESAT-6-specific CD4 T cell responses to aerosol *Mycobacterium tuberculosis* infection are initiated in the mediastinal lymph nodes. Proceedings of the National Academy of Sciences 105: 10961.
42. Bollampalli VP, Yamashiro LH, Feng X, Bierschenk D, Gao Y, Blom H, Henriques-Normark B, Nylén S, and Rothfuchs AG. 2015. BCG Skin Infection Triggers IL-1R-MyD88-Dependent Migration of EpCAMlow CD11bhigh Skin Dendritic cells to Draining Lymph Node During CD4+ T-Cell Priming. PLoS Pathogens 11: e1005206. [PubMed: 26440518]
43. Darrah PA, Zeppa JJ, Maiello P, Hackney JA, Wadsworth MH, Hughes TK, Pokkali S, Swanson PA, Grant NL, Rodgers MA, Kamath M, Causgrove CM, Laddy DJ, Bonavia A, Casimiro D, Lin PL, Klein E, White AG, Scanga CA, Shalek AK, Roederer M, Flynn JL, and Seder RA. 2020. Prevention of tuberculosis in macaques after intravenous BCG immunization. Nature 577: 95–102. [PubMed: 31894150]
44. Olsen AW, Brandt L, Agger EM, Pinxteren LAHV, and Andersen P. 2004. The Influence of Remaining Live BCG Organisms in Vaccinated Mice on the Maintenance of Immunity to Tuberculosis. Scand J Immunol 60: 273–277. [PubMed: 15320884]
45. Andersen P, and Urdahl KB. 2015. TB vaccines; promoting rapid and durable protection in the lung. Curr Opin Immunol 35: 55–62. [PubMed: 26113434]
46. Lu K, Psakhye I, and Jentsch S. 2014. Autophagic clearance of polyQ proteins mediated by ubiquitin-Atg8 adaptors of the conserved CUET protein family. Cell 158: 549–563. [PubMed: 25042851]
47. Reed M, Morris SH, Jang S, Mukherjee S, Yue Z, and Lukacs NW. 2013. Autophagy-inducing protein beclin-1 in dendritic cells regulates CD4 T cell responses and disease severity during respiratory syncytial virus infection. J Immunol 191: 2526–2537. [PubMed: 23894198]
48. Nakahira K, Haspel JA, Rathinam VA, Lee S-J, Dolinay T, Lam HC, Englert JA, Rabinovitch M, Cernadas M, and Kim HP. 2011. Autophagy proteins regulate innate immune responses by inhibiting the release of mitochondrial DNA mediated by the NALP3 inflammasome. Nature immunology 12: 222–230. [PubMed: 21151103]
49. Verhave J, Boucher A, Dandavino R, Collette S, Senecal L, Hebert MJ, Girardin C, and Cardinal H. 2014. The incidence, management, and evolution of rapamycin-related side effects in kidney transplant recipients. Clin Transplant 28: 616–622. [PubMed: 24654608]
50. Ryan TA, Phillips EO, Collier CL, Robinson AJB, Routledge D, Wood RE, Assar EA, and Tumbarello DA. 2020. Tollip coordinates Parkin-dependent trafficking of mitochondrial-derived vesicles. The EMBO Journal 39: e102539. [PubMed: 32311122]
51. Jongsma ML, Berlin I, Wijdeven RH, Janssen L, Janssen GM, Garstka MA, Janssen H, Mensink M, van Veelen PA, Spaapen RM, and Neefjes J. 2016. An ER-Associated Pathway Defines Endosomal Architecture for Controlled Cargo Transport. Cell 166: 152–166. [PubMed: 27368102]
52. Neefjes J, Jongsma MLM, Paul P, and Bakke O. 2011. Towards a systems understanding of MHC class I and MHC class II antigen presentation. Nature Reviews Immunology 11: 823–836.
53. Didierlaurent A, Brissoni B, Velin D, Aebi N, Tardivel A, Kaslin E, Sirard JC, Angelov G, Tschopp J, and Burns K. 2006. Tollip regulates proinflammatory responses to interleukin-1 and lipopolysaccharide. Mol. Cell. Biol 26: 735–742. [PubMed: 16428431]
54. Brissoni B, Agostini L, Kropf M, Martinon F, Swoboda V, Lippens S, Everett H, Aebi N, Janssens S, Meylan E, Felberbaum-Corti M, Hirling H, Gruenberg J, Tschopp J, and Burns K. 2006.

Intracellular trafficking of interieukin-1 receptor I requires Tollip. Curr. Biol 16: 2265–2270. [PubMed: 17113392]

55. Bourgeois-Daigneault M-C, Pezeshki AM, Galbas T, Houde M, Baril M, Früh K, Amrani A, Ishido S, Lamarre D, and Thibodeau J. 2013. Tollip-induced down-regulation of MARCH1. Results in immunology 3: 17–25. [PubMed: 24600555]
56. Esaulova E, Das S, Singh DK, Choreño-Parra JA, Swain A, Arthur L, Rangel-Moreno J, Ahmed M, Singh B, Gupta A, Fernández-López LA, Garcia-Hernandez M. d. l. L., Bucsan A, Moodley C, Mehra S, García-Latorre E, Zuniga J, Atkinson J, Kaushal D, Artyomov MN, and Khader SA. 2020. The immune landscape in tuberculosis reveals populations linked to disease and latency. Cell Host & Microbe.
57. Kauffman KD, Sallin MA, Sakai S, Kamenyeva O, Kabat J, Weiner D, Sutphin M, Schimel D, Via L, Barry CE, Wilder-Kofie T, Moore I, Moore R, and Barber DL. 2018. Defective positioning in granulomas but not lung-homing limits CD4 T-cell interactions with Mycobacterium tuberculosis-infected macrophages in rhesus macaques. Mucosal Immunology 11: 462–473. [PubMed: 28745326]
58. Qualls JE, and Murray PJ. 2016. Immunometabolism within the tuberculosis granuloma: amino acids, hypoxia, and cellular respiration. Seminars in Immunopathology 38: 139–152. [PubMed: 26490974]
59. Ramakrishnan L 2012. Revisiting the role of the granuloma in tuberculosis. Nature Reviews Immunology 12: 352–366.
60. Gasteiger G, Ataide M, and Kastenmüller W. 2016. Lymph node - an organ for T-cell activation and pathogen defense. Immunol Rev 271: 200–220. [PubMed: 27088916]
61. Berry MP, Graham CM, McNab FW, Xu Z, Bloch SA, Oni T, Wilkinson KA, Banchereau R, Skinner J, Wilkinson RJ, Quinn C, Blankenship D, Dhawan R, Cush JJ, Mejias A, Ramilo O, Kon OM, Pascual V, Banchereau J, Chaussabel D, and O'Garra A. 2010. An interferon-inducible neutrophil-driven blood transcriptional signature in human tuberculosis. Nature 466: 973–977. [PubMed: 20725040]
62. Krawczyk CM, Holowka T, Sun J, Blagih J, Amiel E, DeBerardinis RJ, Cross JR, Jung E, Thompson CB, Jones RG, and Pearce EJ. 2010. Toll-like receptor–induced changes in glycolytic metabolism regulate dendritic cell activation. Blood 115: 4742–4749. [PubMed: 20351312]
63. Everts B, Amiel E, Huang SC-C, Smith AM, Chang C-H, Lam WY, Redmann V, Freitas TC, Blagih J, Windt G. J. W. v. d., Artyomov MN, Jones RG, Pearce EL, and Pearce EJ. 2014. TLR-driven early glycolytic reprogramming via the kinases TBK1-IKKε supports the anabolic demands of dendritic cell activation. Nature Immunology 15: 323–332. [PubMed: 24562310]
64. Peters W, Cyster JG, Mack M, Schlöndorff D, Wolf AJ, Ernst JD, and Charo IF. 2004. CCR2-dependent trafficking of F4/80dim macrophages and CD11cdim/intermediate dendritic cells is crucial for T cell recruitment to lungs infected with Mycobacterium tuberculosis. The Journal of Immunology 172: 7647–7653. [PubMed: 15187146]
65. Lapteva N 2010. Enhanced migration of human dendritic cells expressing inducible CD40. Methods Mol Biol 651: 79–87. [PubMed: 20686961]
66. Poyntz HC, Stylianou E, Griffiths KL, Marsay L, Checkley AM, and McShane H. 2014. Non-tuberculous mycobacteria have diverse effects on BCG efficacy against Mycobacterium tuberculosis. Tuberculosis (Edinb) 94: 226–237. [PubMed: 24572168]
67. Whang MI, Tavares RM, Benjamin DI, Kattah MG, Advincula R, Nomura DK, Debnath J, Malynn BA, and Ma A. 2017. The Ubiquitin Binding Protein TAX1BP1 Mediates Autophagasome Induction and the Metabolic Transition of Activated T Cells. Immunity 46: 405–420. [PubMed: 28314591]
68. Chi H 2012. Regulation and function of mTOR signalling in T cell fate decisions. Nature Reviews Immunology 12: 325–338.

Key Points

- A functionally active SNP in the TOLLIP promoter is associated with decreased IL-12.
- TOLLIP participates in DC maturation during *M. tuberculosis* infection.

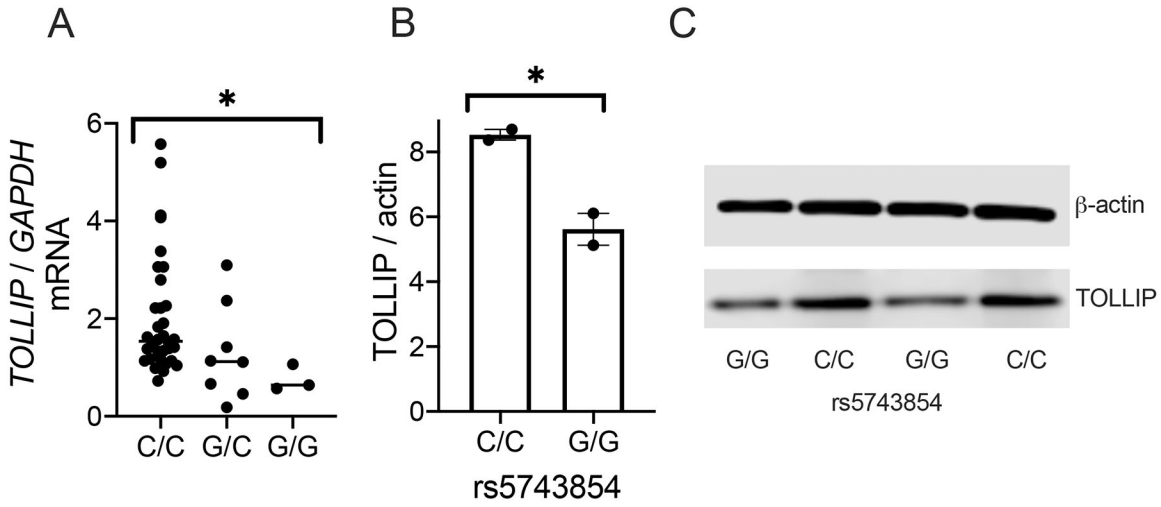

Figure 1. SNP rs5743854 is associated with diminished TOLLIP expression in monocyte-derived DC.

A) *TOLLIP* mRNA expression, normalized to *GAPDH*, was measured from RNA extracted from monocyte-derived DC isolated from healthy volunteers and stratified by rs5743854. N = 34 C/C genotype, 8 G/C genotype, and 3 G/G genotype. Data are presented as scatterplots with bars indicating median values. Each dot represents mRNA expression from a single study participant. * $p < 0.05$, generalized linear model.

B-C) TOLLIP protein expression, normalized to β-actin, was measured in bone marrow-derived DC isolated from two individuals with C/C and G/G genotypes, respectively. B) Western blot images and C) semiquantitative measurement of normalized protein expression. Bars represent mean values. * $p < 0.05$, standard two-sided t-test. Each experiment was performed at least twice; all data are shown.

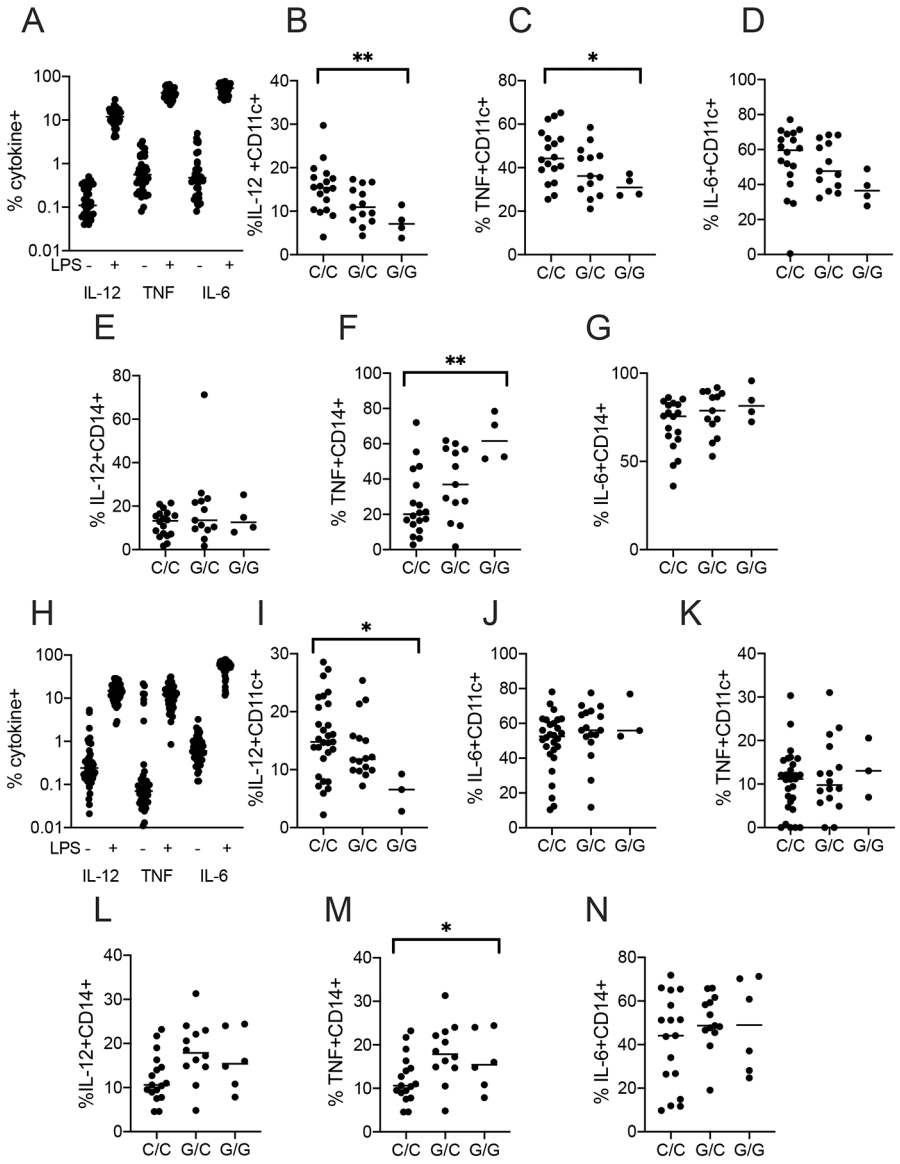

Figure 2. TOLLIP SNP rs5743854 allele G is associated with decreased LPS-induced cytokine responses in peripheral blood DC.

A) Proportion of peripheral blood DC (MHC-II+CD14-CD16-CD11c+) producing cytokines of interest from healthy volunteers (N=35), after media or LPS stimulation. Whole blood was drawn from healthy donors and immediately stimulated with LPS (10 ng/ml) for 6 hours in the presence of BFA and monensin.

B-D) Proportion of CD11c+ DC producing C) IL-12, D) TNF, or E) IL-6, stratified by SNP rs5743854.

E-G) Proportion of CD14+ monocytes producing F) IL-12, G) TNF, or H) IL-6, stratified by SNP rs5743854. N = 18 C/C genotype, 13 G/C genotype, and 4 G/G genotype.

H) Proportion of peripheral blood DC (n = 48) producing IL-12, TNF, or IL-6 after media or LPS (10ng/ml) stimulation in a second cohort for 24 hours.

I-K) Proportion of peripheral blood DC producing C) IL-12, D) TNF, or E) IL-6, stratified by SNP rs5743854.

L-N) Proportion of peripheral blood monocytes producing F) IL-12, G) TNF, and H) IL-6, stratified by SNP rs5743854. N = 29 C/C genotype, 16 G/C genotype, and 3 G/G genotype. Data are presented as scatterplots with bars indicating median value. We assessed statistical significance in each graph using a simple generalized linear model, encompassing all data in each subfigure. Graphs lacking bars had a p-value >0.05 using this statistical test. Each dot represents an overall measurement of the proportion of cytokine-producing cells from a single individual. *$p < 0.05$, **$p < 0.01$. Each experiment was performed at least twice; all data are shown.

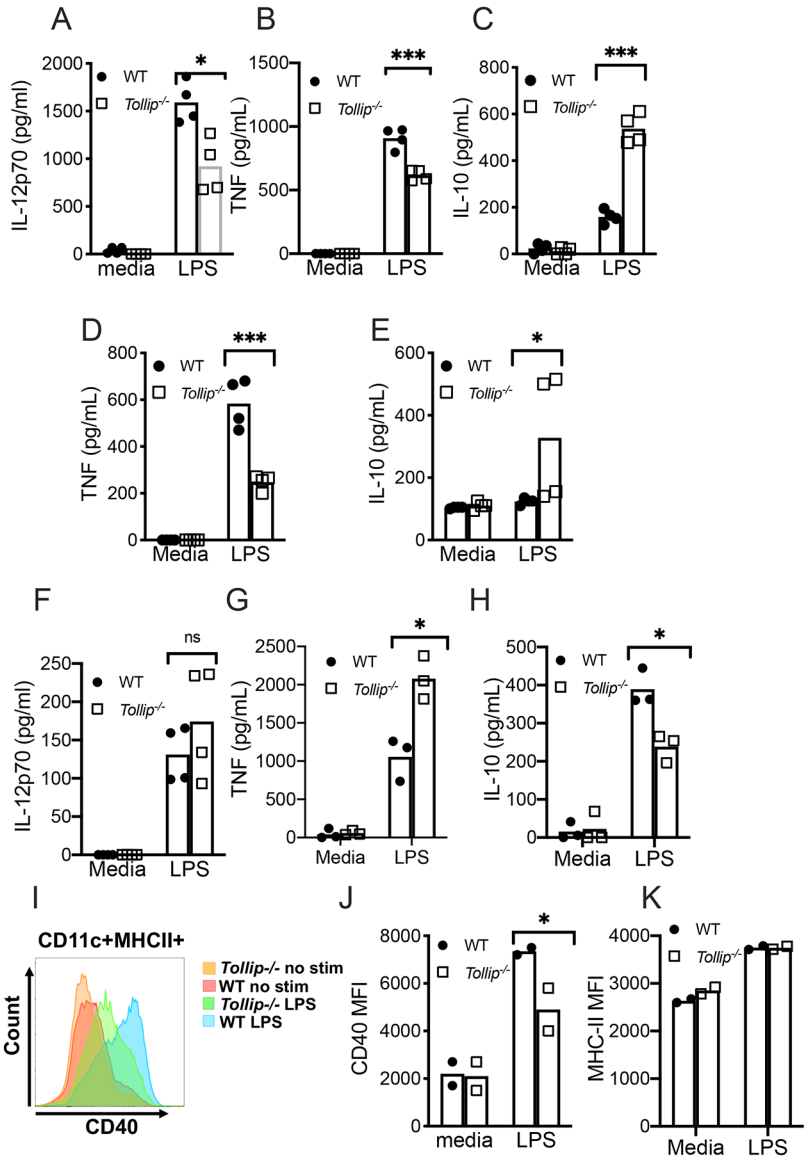

Figure 3. LPS-stimulated *Tollip*$^{-/-}$ DCs mature improperly.

A-C) Bone marrow-derived DC (BMDC), differentiated with IL-4 and GM-CSF treatment for five days, from B6 (*black* bars) and *Tollip*$^{-/-}$ (*gray* bars) mice were treated for 24 hours with media or LPS (10ng/ml). Cellular supernatants were collected and A) IL-12p70, B) TNF, and C) IL-10 concentrations were measured by ELISA.

D-E) BMDC, differentiated with Flt3L treatment for 7 days, from B6 (*black* bars) and *Tollip*$^{-/-}$ (*gray* bars) mice were treated for 24 hours with media or LPS (10ng/ml). Cellular supernatants were collected and D) TNF, and E) IL-10 concentrations were measured by ELISA.

D-F) Bone marrow-derived macrophages (BMDM) from WT and *Tollip*$^{-/-}$ mice were treated for 24 hours with medial or LPS (10ng/ml). Cellular supernatants were collected and D) IL-12p70, E) TNF and F) IL-10 concentrations were measured by ELISA.

G-H) Cell surface CD40 expression was measured by flow cytometry from WT and *Tollip*$^{-/-}$ BMDC. G) Histograms of CD40 expression after media or LPS stimulation and H) median fluorescence intensity (MFI) for CD40.

I) H-2b (MHC-II) MFI after media or LPS stimulation.

*p < 0.05, **p < 0.01, ***p < 0.001, unpaired t-test. Dots represent individual values from a single experimental replicate. Error bars represent SEM. Data are representative of at least two independent experiments. All data are shown.

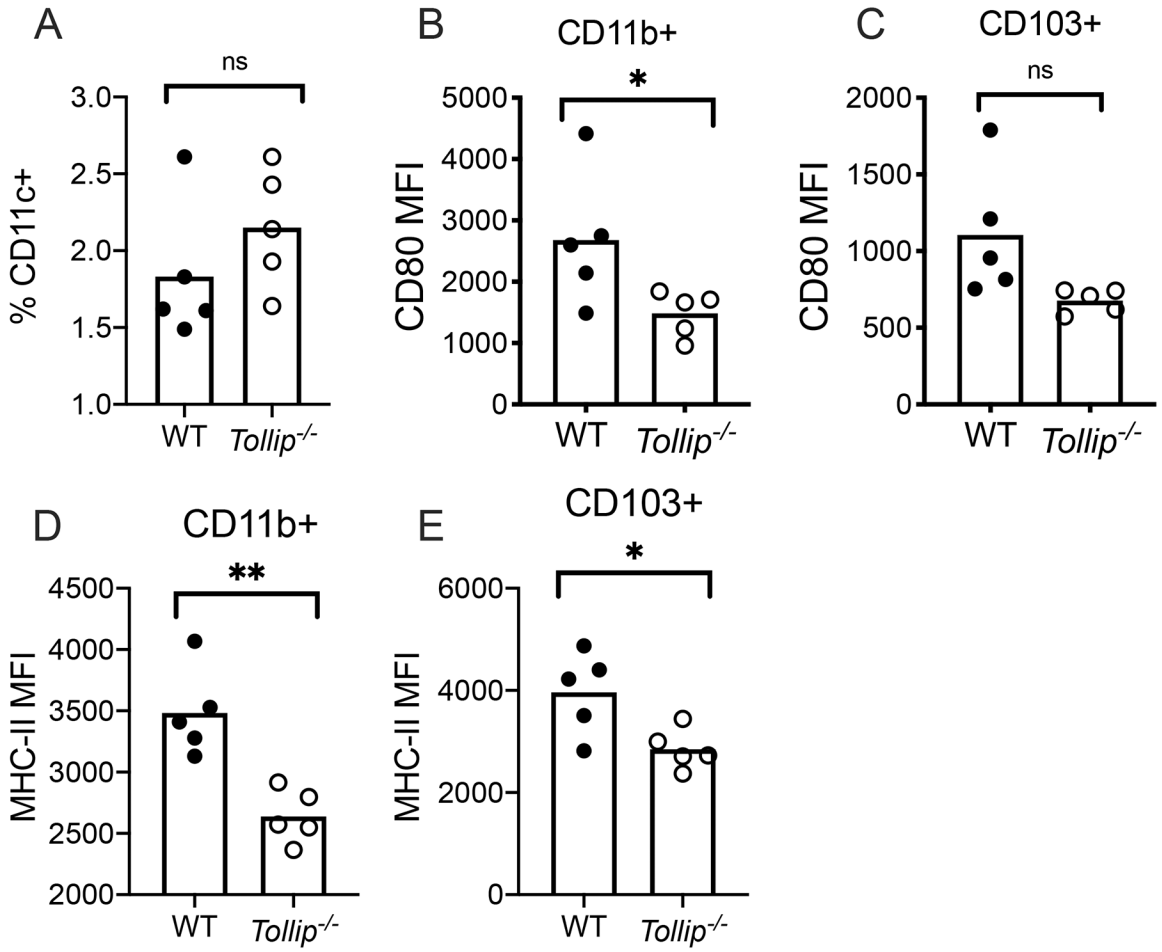

Figure 4. DCs from *Tollip*$^{-/-}$ mice demonstrate diminished CD80 expression during Mtb infection.

WT and *Tollip*$^{-/-}$ mice were infected with Mtb H37Rv strain via the aerosol method (50 CFU). Single cell homogenates of lung tissue were obtained 28 days after infection and DC populations were characterized. WT DC (*black* circles) were compared to *Tollip*$^{-/-}$ (*clear* circles) DC. Bars represent mean values.

A) Frequency of overall DC (MHCII+Ly6G-SiglecF-CD11c+) among total lung cell populations (live singlets) 28 days after Mtb infection.

B-C) Median fluorescence intensity (MFI) of CD80 on B) CD11b+ DC (MHCII+Ly6GSiglecF-CD11c+CD11b+) and C) CD103+ DC (CD103+CD11c+MHCII+CD11b-Ly6G-SiglecF-).

D-E) MHC Class II (H-2b) MFI on D) CD11b+ (MHCII+Ly6GSiglecF-CD11c+CD11b+) and E) CD103+ DC (CD103+CD11c+MHCII+CD11b-Ly6G-SiglecF-) by genotype. *p < 0.05, **p < 0.01, ***p < 0.001, unpaired t-test. Bars represent mean values. Dots represent individual values from a single experimental replicate. Data are representative of at least two independent experiments. All data are shown.

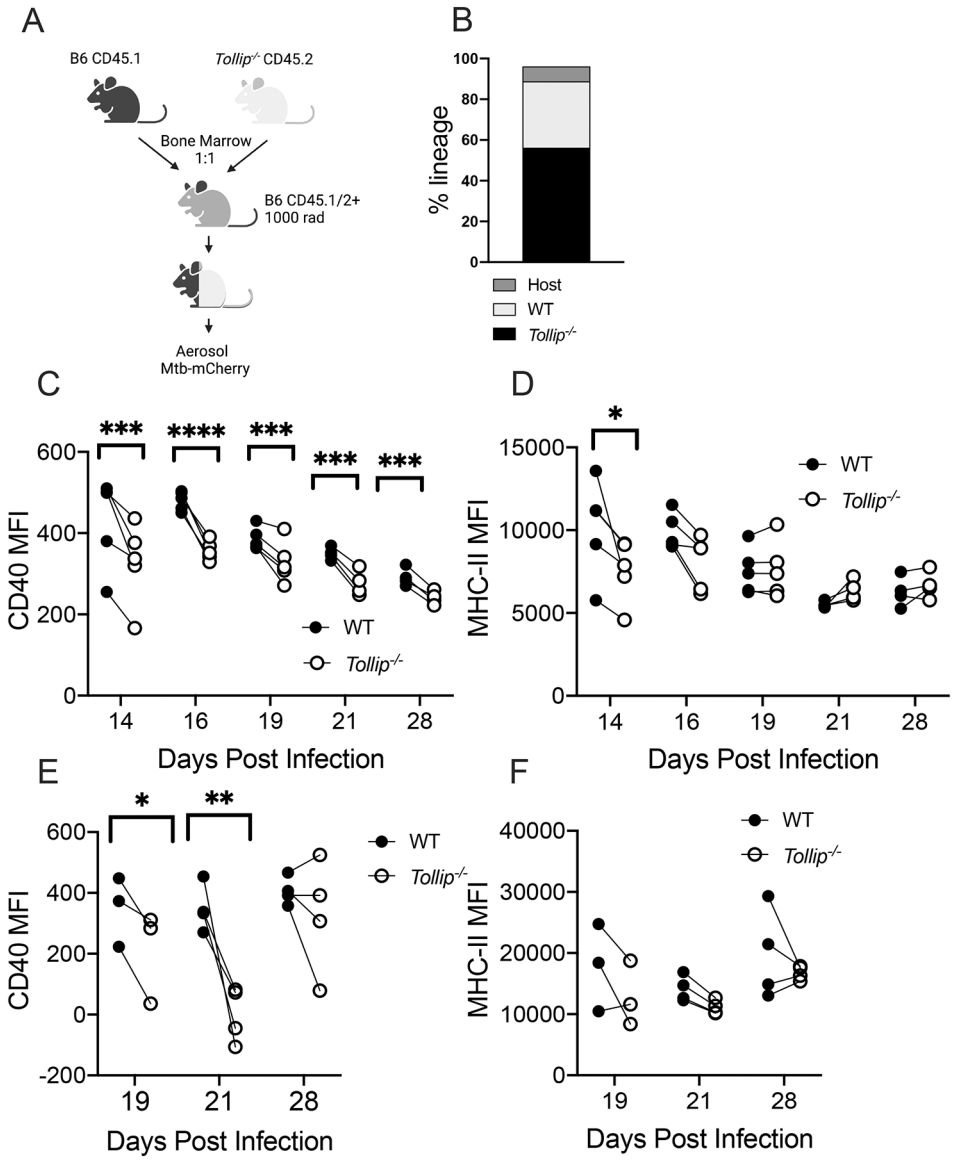

Figure 5. TOLLIP contributes to DC maturation during Mtb infection.

WT:*Tollip*$^{-/-}$ mixed bone marrow chimeric mice were infected with H37Rv Mtb expressing mCherry (50 CFU) via aerosol and DC were assessed 19, 21, and 28 days after infection in lungs and draining LN. *Black circles* are WT DC, and *clear circles* are *Tollip*$^{-/-}$ DC.

A) Experimental strategy and timeline.

B) Frequency of CD45.1 and CD45.2 expression from the whole blood of mixed bone marrow chimeric mice.

C) CD40 median fluorescence intensity (MFI) in MHCII+CD11c+SiglecF-Ly6G-CD11b+ (CD11b+) lung DCs from mixed bone marrow chimeric mice by genotype.

D) MFI of MHCII (H-2b) expression in CD11b+ lung DCs from mixed bone marrow chimeric mice.

E) MFI of CD40 expression in CD11b+ MLN DCs from mixed bone marrow chimeric mice.

F) MFI of MHCII (H-2b) expression in CD11b+ MLN DCs from mixed bone marrow chimeric mice.

*p<0.05, ** p<0.01, *** p < 0.001; **** p < 0.0001. paired two-sided t-test, n = 3–5 mice/group. Experiments were performed at least four times. Dots represent pooled data from each lineage, connected by a line with data from the other lineage from the same mouse. All data are shown.

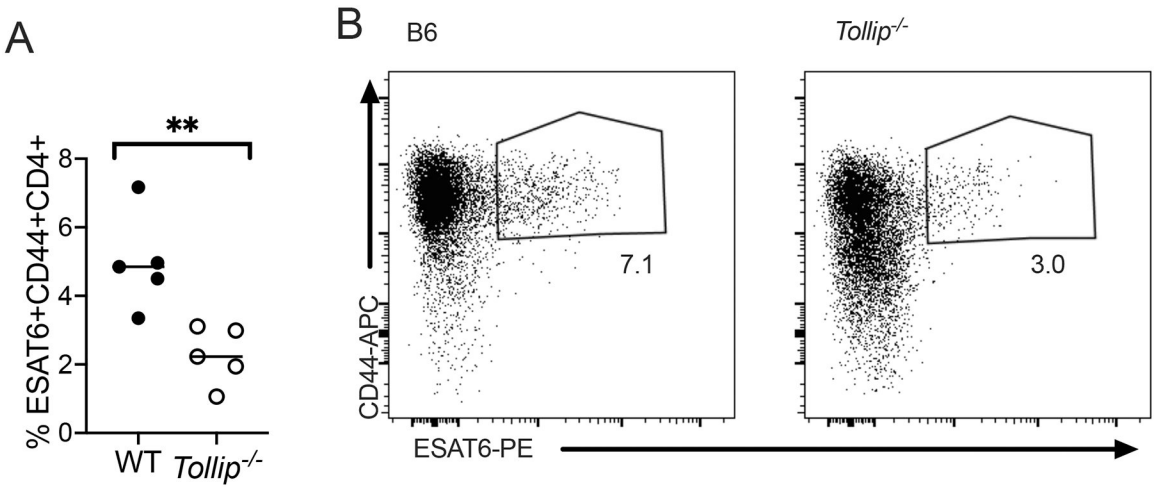

Figure 6. *Tollip*$^{-/-}$ mice develop fewer Mtb-specific CD4+ T cells after infection.

Mice were infected with Mtb via the aerosol route (50 CFU) and 28 days after infection, lungs were homogenized and the frequency of ESAT-6+ cells was measured via tetramer staining.

A-B) Frequency of ESAT-6+CD44+CD4+ T cells (A) in the lungs and (B) a representative image of tetramer staining by flow cytometry. Each experiment was performed at least twice; all data are shown.

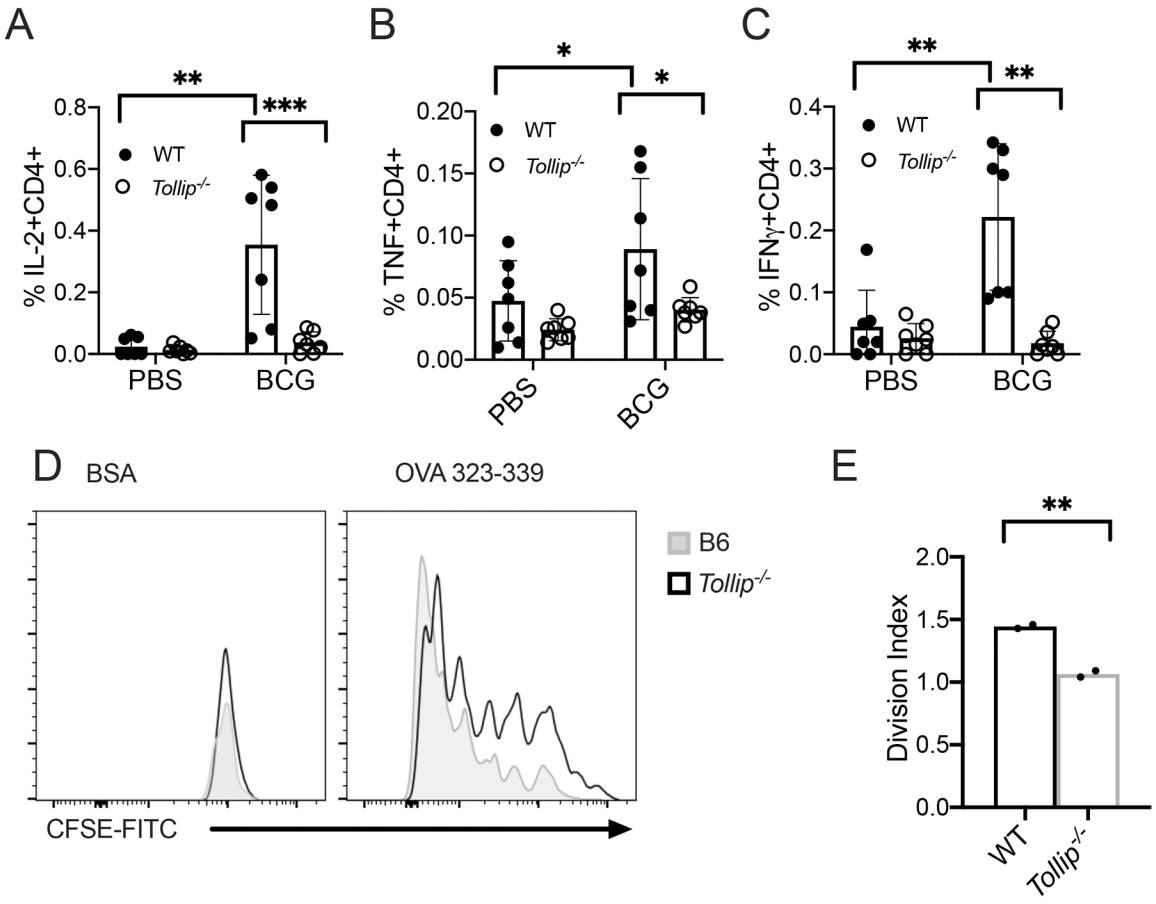

Figure 7. TOLLIP is required for development of BCG-specific CD4+ T cell responses after intravenous BCG vaccination.

WT and *Tollip*$^{-/-}$ mice were vaccinated with 10^6 CFU of BCG Russia strain via the intravenous route. Two months after vaccination, splenocytes were harvested and CD4+ T cell responses were assessed by restimulating splenocytes with overlapping pooled peptides of Ag85A and Ag85B. WT samples are shown with *black circle*s and *Tollip*$^{-/-}$ samples are shown with *clear circles*.

A-C) Frequency of A) IL-2+, B) TNF+, and C) IFNγ+ CD4+ T cells after Ag85A and Ag85B peptide restimulation. Samples are corrected for background staining (cytokine+ T cell frequency from Ag85A/B group – cytokine+ T cells from control). N = 8. Experiments were performed at least twice; all data are shown. Statistical significance was determined by two-sided t-test comparing PBS vaccination with BCG vaccination state in each genotype. Bars indicate mean values.

D-E) Representative histograms (D) of CFSE expression and division index (E; the average number of cell divisions) by OVA-specific CD4+ T cells seven days after coincubation with BMDC and OVA323–339 peptide or BSA control. *p < 0.05, **p < 0.01, ***p < 0.001, unpaired t-test. Error bars represent SEM. Data are representative of at least two independent experiments. All data are shown.

Table 1.

Clinical Characteristics

Cohort	Cohort 1	Cohort 2
Female, N (%)	17 (50)	22 (47)
Ethnicity/Race, N (%)		
White	20 (59)	33 (70)
Asian	7 (21)	9 (19)
Black/African American	1 (3)	1 (2)
Multiple	2 (6)	1 (2)
Unknown or did not disclose	2 (6)	3 (6)
Latinx	1 (3)	0 (0)
Age at Blood Collection, Median+/− IQR *	38 (25 – 55)	37 (27 – 49)

* IQR – intraquartile range